Heterodyne detection of multiply scattered monochromatic light with a multipixel detector

M. Gross and P. Goy

Laboratoire Kastler Brossel de l'Ecole Normale Superieure et de l'Université Pierre et Marie Curie associé au le Centre National de la Recherche Scientifique, Unité Mixte de Recherche 8552, 24 Rue Lhomond, F-75231 Paris Cedex 05, France

B. C. Forget, M. Atlan, F. Ramaz, and A. C. Boccara

Laboratoire d'Optique, Ecole Supérieure de Physique et de Chimie Industrielles de la Ville de Paris, Centre National de la Recherche Scientifique, Unité Propre de Recherche A0005, Université Pierre et Marie Curie, 10 Rue Vauquelin, 75231 Paris Cedex 05, France

A. K. Dunn

Martinos Center for Biomedical Imaging, Massachusetts General Hospital, Charlestown, Massachusetts 02114

Received November 5, 2004

A new technique is presented for measuring the spectral broadening of light that has been multiply scattered from scatterers in motion. In our method the scattered light is detected by a heterodyne receiver that uses a CCD as a multipixel detector. We obtain the frequency spectrum of the scattered light by sweeping the heterodyne local oscillator frequency. Our detection scheme combines a high optical etendue (product of the surface by the detection solid angle) with an optimal detection of the scattered photons (shot noise). Using this technique, we measure, *in vivo*, the frequency spectrum of the light scattered through the breast of a female volunteer. © 2005 Optical Society of America

OCIS codes: 290.3700, 290.7050, 170.3340, 170.6480, 170.3830.

We are involved in the development of acousto-optic imaging techniques for thick biological tissues[1] (e.g., breast imaging), in which the temporal evolution of the speckle is an important limitation of the performance. To analyze the speckle, we developed a technique, inspired by a previous work,[2] that is able to perform optimal, shot-noise-limited, heterodyne detection of scattered light on a two-dimensional (2D) detector. We have used our method to measure, *in vivo*, the frequency spectrum of the light scattered through the breast of a female volunteer. In addition to acousto-optic imaging of biological tissue, the technique presented in this Letter is applicable to the general field of dynamic light scattering.

Coherent light (laser) scattering from moving objects or particles produces intensity fluctuations that can be used to measure the spectral (Doppler) broadening caused by the motion of the scatterers. Two equivalent approaches[3] have been used to analyze these fluctuations: laser Doppler and time-varying speckle analysis. In laser Doppler analysis (see introduction to feature issues in Applied Optics[4,5]) the scattered light is detected in the far field by a single detector (photodiode or photomultiplier) and analyzed by a correlator or a spectrum analyzer. The sensitivity can be very high, in particular when the scattered light is mixed with a local oscillator (LO) beam.[6] However, the optical etendue (product of the surface area and the detection solid angle) is low because the scattered light is collimated with pinholes or optical fibers.[7] In speckle contrast analysis techniques the scattering object is imaged, without mixing (self-beating detection), on the detector, which can be advantageously 2D (photographic plate,[8] CCD,[9] or complementary metal-oxide semiconductor camera[10]). Accounting for the space–time relationship of the correlation functions,[11] one can determine information about the motion of the scatterers.[10,12–14] With 2D detection, speckle techniques benefit from a high etendue but do not benefit from the LO beam mixing. Our technique combines the advantages of laser Doppler with LO beam mixing (high sensitivity) and speckle analysis (high etendue).

Figure 1 shows the experimental setup. The 780-nm, 50-mW beam of the laser (Sanyo DL-7140-201, current of 95 mA) is split into two beams. The main (>90% of the power) beam (frequency ν_L) is scattered by the sample (signal beam). The lower-intensity beam (<10%) is the LO of the CCD heterodyne detection. The respective power of the two beams is adjusted by moving the adjustable mirror. By use of acousto-optic modulators AOM1 and AOM2 (Crystal Technology, $\nu_{\mathrm{AOM1,2}} \simeq 80$ MHz), LO beam frequency ν_{LO} can be freely adjusted: $\nu_{\mathrm{LO}} = \nu_L + (\nu_{\mathrm{AOM1}} - \nu_{\mathrm{AOM2}})$. Two numerical synthesizers with the same 50-MHz quartz reference clock provide the $\nu_{\mathrm{AOM1,2}}$ rf signals. Lens L (25 mm) focuses the LO beam at an equiva-

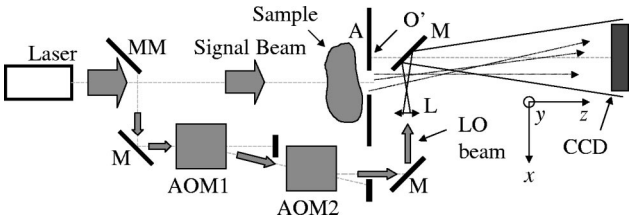

Fig. 1. Experimental setup: MM, adjustable mirror; M's, mirrors; L, short focal lens; A, rectangular aperture.

0146-9592/05/111357-3/$15.00

lent point O′ located in the plane of vertical slit A (width of 5.5 mm) 1.3 cm from the center of the slit. The LO plus signal interference pattern is recorded by the CCD camera (PCO Pixelfly, digital 12 bits, $\nu_{CCD}=12.5$ Hz, exposure time of 80 ms, with 1280 $\times$1024 pixels of 6.7 μm$\times$6.7 μm), which is typically located 30 cm from the slit. The camera is used in $\times 4$ vertical binning mode (50 Hz, 1280×256).

Because of the LO beam spatial coherence, the CCD camera records digital holograms.[15] By choosing $\nu_{LO}=\nu_L+\nu_{CCD}/4$, we recorded sequences of four CCD images ($I_0 \ldots I_3$) and calculated the complex field E (i.e., the complex hologram) by the four-phase heterodyne variant[16] of the phase-shifting method[17]: $E=(I_0-I_2)+j(I_1-I_3)$. We calculated field E' in the plane of slit A; i.e., we reconstructed the image of A (which is backilluminated by light diffused by the sample located 2 cm behind A). Because O′ is within the A plane, the calculation of E' is made with a simple 2D Fourier transform: $E'=\mathrm{FT}_{x,y}(E)$.

Figure 2(a) shows in logarithmic scale the intensity image ($|E'|^2$) obtained with a highly diffusing scattering sample [10% polyvinyl alcohol (PVA) in water, scattering coefficient $\mu_s=3.9$ cm^{-1}, thickness of 3 cm]. The scatterers are not moving, and the scattered photons remain within the $\nu=\nu_L$ frequency delta function. The heterodyne detection, whose bandwidth is narrow ($\approx\nu_{CCD}$), is fully efficient. The image of the aperture (1) is bright. By making the heterodyne detection on the other sideband (with $\nu_{LO}=\nu_L-\nu_{CCD}/4$), one gets a reversed image, with the aperture on the left-hand side. The twin image[15] seen in 2 thus corresponds to the $\nu_{LO}-\nu_{CCD}/4=\nu_L-\nu_{CCD}/2$ signal. It is low because the scatterers are not moving ($\nu=\nu_L$ delta function). The zeroth-grating-order (3) parasitic image corresponds to the the LO beam. It is low because the LO contributions cancel out in the four-phase calculation of E.

In Fig. 2(b) the sample is the hand of one of the authors: the main beam traveled through the medius–ring finger commissure (5 mm thick). The motion of the scatterers (blood flow) Doppler broadens the scattered light (measured half-width $\approx$300 Hz). The heterodyne detection is less efficient, and the brightness of the aperture image (1) is lower. Moreover, approximately the same signal level is obtained on the two heterodyne sidebands ($\nu_{LO}\pm\nu_{CCD}/4$), and the twin image (2) is as bright as the image itself (1). The zeroth-grating-order parasite (3) is still low.

To make a quantitative measurement of the scattered light signal, we plotted sum $S(x)$ of the intensity signal over the y axis: $S(x)=\int|E'(x,y)|^2\mathrm{d}y$ (Fig. 3). With the PVA sample (a) the rectangular peak of the aperture (arrow 1) is much higher. With the hand (b) the aperture peaks (arrows 1 and 2) are lower and roughly symmetric. The zeroth-order parasites (arrow 3) correspond to an excess noise of several orders of magnitude but in a localized region.

To explore the Doppler profile of the scattered photons, the frequency of the LO beam, $\nu_{LO}-\nu_L=\Delta\nu$ was offset by values of 0, 0.1, 0.3, and 1 kHz (c, d, e, and f, respectively, in Fig. 4). To obtain a better signal, we recorded sequences of two images (I_0,I_1) and calculated two phase holograms ($E=I_0-I_1$). We then averaged the intensity data ($|E'|^2$) over 64 sequences. As seen in Fig. 4, the scattered photon signal (arrows 1 and 2) decreases with the offset.

The signal observed in the regions masked by the aperture (arrows 4 and 5) is very flat. It is roughly the same as without a signal (with the LO beam alone). Considering the PCO camera gain of 2.4e (photoelectrons) per count (saturation corresponds to 4096 counts), the signal level is within 10% of the LO beam shot noise. Here the shot noise corresponds, on the signal beam, to 1e per pixel (or per field mode) within measurement time T_m and measurement bandwidth $1/T_m$. Therefore the noise floor provides an absolute calibration of the signal. As an example, on curve c in Fig. 4 the noise floor (arrows 4 and 5) is 1e; the signal (arrows 1 and 2) is 2e; and the signal, after noise correction and calibration, is $S'=2-1=1e$.

To illustrate the ability of our technique to obtain pertinent information with a very low signal, we recorded the frequency spectrum of the light transitted through the breast of a female volunteer (4-cm thickness). The breast was gently pressed between two transparent poly(methyl methacrylate) plates, and a Hitachi KPF2B (658×496 pixels of 7.4 μm$\times$7.4 μm,

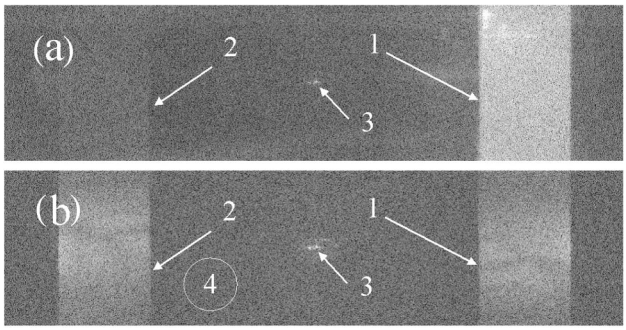

Fig. 2. Aperture-reconstructed image by a 1024×256 fast Fourier transform: The 1280×256 CCD pixels have been truncated to 1024×256. The main beam is diffused by (a) a PVA sample and (b) a hand.

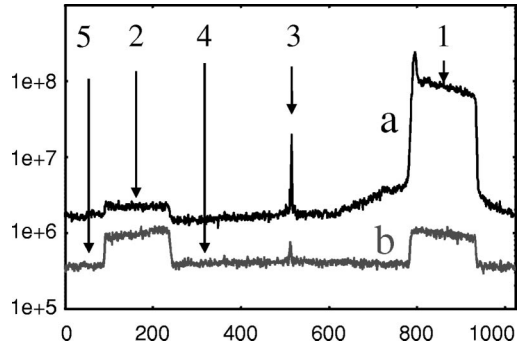

Fig. 3. Sum $S(x)$ over the y axis of the images of Fig. 2 for the PVA sample (curve a) and the hand (curve b). The horizontal scale is pixels in the 1024×256 fast Fourier transform calculation grid (512 correspond to the zeroth spatial frequency).

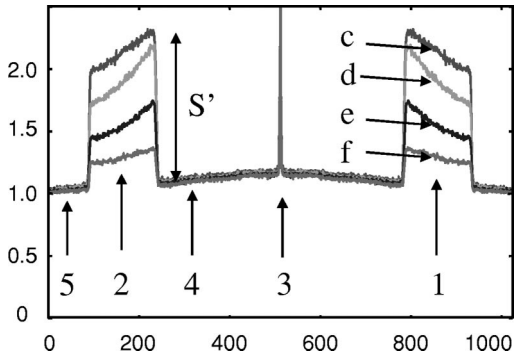

Fig. 4. Sum $S(x)$ for the hand with a LO frequency offset $\Delta\nu=0$, 0.1, 0.3, and 1 kHz (c, d, e, and f, respectively). Same horizontal scale as in Fig. 3.

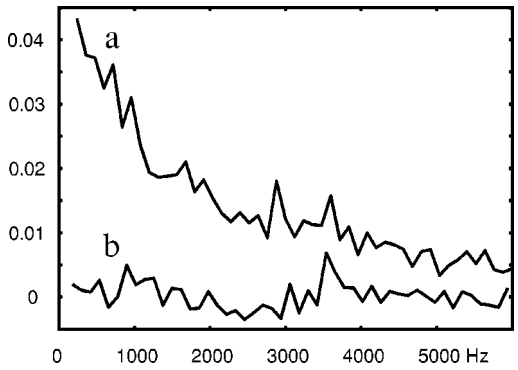

Fig. 5. Curve a, frequency spectrum of the light diffused by the breast ($\Delta\nu=0\ldots6$ kHz); curve b, zero signal reference ($\Delta\nu=10\ldots16$ kHz).

quantum efficiency of 25% at 780 nm, exposure time of 16 ms) analog CCD camera was used. A Matrox Meteor frame grabber grabbed the odd line images (640×240 pixels) continuously at $\nu_{\mathrm{CCD}}=60$ Hz.

A total of 12,800 images were grabbed in 213 s while $\Delta\nu$ was swept from 0 to 6 kHz in 100 frequency intervals, each corresponding to 64 sequences of 2 images: $100\times64\times2=12{,}800$. Half of the frequencies were overoffset by 10 kHz ($\Delta\nu=10\ldots16$ kHz). Since this offset is large with respect to the observed half-linewidth (1.5 kHz), one obtains a reference level far from the resonance.

For each sequence, $S(x)$ was calculated from the two-phase detection. For each frequency we averaged $S(x)$ over the 64 sequences: $\langle S(x)\rangle=(1/32)\Sigma S(x)$. We obtained the signal plus noise spectral component $P_{S+N}(\Delta\nu)$ of the scattered light by summing $\langle S\rangle$ over the x interval that corresponds to aperture region 1: $P_{S+N}=\int_1 dx\langle S(x)\rangle$. We obtain noise component P_N by summing over an equal size interval that corresponds to a flat region such as those indicated by arrows 4 and 5.

Figure 5 shows the $\Delta\nu$ frequency spectrum of the light diffused by the breast. Curve a shows the signal after noise correction and calibration: $P_S=(P_{S+N}-P_N)/P_N$, and curve b shows the reference level. At maximum ($\Delta\nu=0$) the signal is $\approx0.05\times$ the shot noise (1e per CCD pixel within 33 ms and 30 Hz), and the signal-to-noise ratio is ≈5. We observe a spectrum with a half-width of ≈1.5 kHz. This width is comparable with that obtained in Ref. 18 on a human wrist. This result is important for acousto-optic imaging,[1,18,19] in particular for its application to breast imaging.

In conclusion, we have achieved a study of light scattered by thick living biological tissue with optimal (shot-noise) sensitivity and with high etendue owing to the parallel detection on a large number of detectors (pixels of a CCD camera). Our technique is frequency selective with a bandwidth fixed by the camera frame rate. The detection frequency is controlled by the AOM and can easily be scanned to obtain a frequency profile of the scattered light. An added advantage of using our technique is that the alignment of our setup is easy. With a multipixel detector there is no restrictive mode-matching condition. The LO beam is within one or a few modes, and the detection is made over all the modes supported by the multipixel detector.

M. Gross's e-mail address is gross@lkb.ens.fr.

References

1. S. Lévêque, A. C. Boccara, M. Lebec, and H. Saint-Jalmes, Opt. Lett. **24**, 181 (1999).
2. M. Gross, P. Goy, and M. Al-Koussa, Opt. Lett. **28**, 2482 (2003).
3. J. Briers, J. Opt. Soc. Am. A **13**, 345 (1996).
4. W. V. Meyer, A. E. Smart, R. G. W. Brown, and M. A. Anisimov, Appl. Opt. **36**, 7477 (1997).
5. W. V. Meyer, A. E. Smart, and R. G. W. Brown, Appl. Opt. **40**, 3965 (2001).
6. R. Brown, Appl. Opt. **40**, 4004 (2001).
7. R. Brown, Appl. Opt. **26**, 4846 (1987).
8. A. Fercher and J. Briers, Opt. Commun. **37**, 326 (1981).
9. J. Briers and S. Webster, Opt. Commun. **116**, 36 (1995).
10. A. Serov, W. Steenbergen, and F. de Mul, Opt. Lett. **27**, 300 (2002).
11. T. Yoshimura, J. Opt. Soc. Am. A **3**, 1032 (1986).
12. N. Takai, T. Iwai, T. Ushizaka, and T. Asakura, Opt. Commun. **30**, 287 (1979).
13. A. F. Fercher, Opt. Commun. **33**, 129 (1980).
14. P. Starukhin, S. Ulyanov, E. Galanzha, and V. Tuchin, Appl. Opt. **39**, 2823 (2000).
15. U. Schnars and W. Jüptner, Appl. Opt. **33**, 179 (1994).
16. F. LeClerc, L. Collot, and M. Gross, Opt. Lett. **25**, 716 (2000).
17. I. Yamaguchi and T. Zhang, Opt. Lett. **22**, 1268 (1997).
18. A. Lev and B. Sfez, J. Opt. Soc. Am. A **20**, 2347 (2003).
19. L. Wang, S. Jacques, and X. Zhao, Opt. Lett. **20**, 629 (1995).